2023-07-12

Efficient Delivery of Biological Cargos into Primary Cells by Electrodeposited Nanoneedles via Cell-Cycle-Dependent Endocytosis

Wang, Z

10.1021/acs.nanolett.2c05083
Nano Letters
American Chemical Society

Efficient delivery of biological cargos into primary cells by electrodeposited nanoneedles via cell cycle-dependent endocytosis

Zongjie Wang[1,2], Hansen Wang[2], Sichun Lin[2,3], Mahmoud Labib[4], Sharif Ahmed[1], Jagotamoy Das[4], Stephane Angers[2,3], Edward H. Sargent[5] and Shana O. Kelley[1,2,4,6,7,8,9,10]*

[1]Department of Biomedical Engineering, McCormick School of Engineering, Northwestern University, Evanston, IL, 60208, USA. [2]Department of Pharmaceutical Sciences, Leslie Dan Faculty of Pharmacy, University of Toronto, Toronto, M5S 3M2, Canada. [3]Terrence Donnelly Centre for Cellular & Biomolecular Research, University of Toronto, Toronto, M5S 3E1, Canada. [4]Department of Chemistry, Weinberg College of Arts & Sciences, Northwestern University, Evanston, IL, 60208, USA. [5]The Edward S. Rogers Sr. Department of Electrical & Computer Engineering, University of Toronto, Toronto, M5S 3G4, Canada. [6]Department of Biochemistry, Feinberg School of Medicine, Northwestern University, Chicago, IL, 60611, USA. [7]International Institute for Nanotechnology, Northwestern University, Evanston, IL, 60208, USA. [8]Robert H. Lurie Comprehensive Cancer Center, Northwestern University, Chicago, IL, 60611, USA. [9]Simpson Querrey Institute, Northwestern University, Chicago, IL, 60611, USA. [10]Chan Zuckerberg Biohub Chicago, Chicago, IL, 60607, USA.

Correspondence to: shana.kelley@northwestern.edu

ABSTRACT

Nanoneedles are a useful tool for delivering exogenous biomolecules to cells. Although therapeutic applications have been explored, the mechanism regarding how cells interact with nanoneedles remains poorly studied. Here, we present a new approach for the generation of nanoneedles, validated their usefulness in cargo delivery, and studied the underlying genetic modulators during delivery. We fabricated arrays of nanoneedles based on electrodeposition and quantified its efficacy of delivery using fluorescently labeled proteins and siRNAs. Notably, we revealed that our nanoneedles caused the disruption of cell membranes, enhanced the expression of cell-cell junction proteins, and downregulated the expression of transcriptional factors of NFkB pathways. This perturbation trapped most of the cells in G2 phase, in which the cells have the highest endocytosis activities. Taken together, this system provides a new model for the study of interactions between cells and high-aspect-ratio materials.

KEYWORDS

Electrodeposition, nanostructure, intracellular delivery, mechanobiology, cell cycle

The delivery of exogenous biomolecules into cells is the foundation of genome editing and cell therapy.[1] Existing approaches often involve the use of viruses, electric fields, or chemicals that are either dangerous, toxic, or inefficient.[2] Hence, there is an unmet need of developing efficient and cost-effective methods for intracellular delivery with minimal cytotoxicity and cellular stress.

Microneedles with a feature size of 100 – 500 μm have demonstrated functionality for intracellular delivery. However, the delivery efficacy via microneedles is usually low (8%[3,4] – 20%[5]) through passive diffusion. In addition, some efforts have been paid to actively deliver plasmids into the cells through microneedle-mediated electroporation.[6] Although the efficacy was boosted to 50%, the setup requires a high voltage (> 50V) to operate.

In contrast, high-aspect-ratio nanomaterials, especially vertical nanoneedles with a feature size of 100 – 1000 nm, have demonstrated a broad utility, efficiency (up to 95%), and minimal cytotoxic effect in intracellular delivery *in vitro*,[7] including nucleic acids,[8] nanoparticles,[9] therapeutic drugs,[10] proteins,[11] and metabolites.[12] In addition, nanoneedles have been introduced for *in situ* gene/immune therapy[13,14] in animal models and achieved encouraging results *in vivo*. Nanoneedles may prove to be a safe and effective tool for intracellular delivery.

Despite the success at the laboratory level, the translation of nanoneedles from bench to clinic is very limited. Several key challenges remain unsolved. Indeed, the fabrication of nanoneedles commonly involves the use of reactive-ion etching (RIE),[2,8–10,12,13,15] which is expensive, non-scalable, labor-intensive, and requires access to the centralized cleanroom facility. The use of RIE significantly hampers the large-scale manufacturing of nanoneedles. Moreover, prior studies have utilized established cancer cell lines to measure/demonstrate the delivery activities, such as leukemic lymphocytes,[16,17] and adherent carcinoma.[8,9,13,16,18] These cancer cell lines are generally easy to transfect and therefore are not a good representation of the primary or stem cells used as therapeutics.[19]

Moreover, the principle of nanoneedle-mediated intracellular delivery is not systematically understood. It has been proposed in some studies that nanoneedles

simply penetrate the cell membrane through membrane disruption[2,12,20,21] while others suggest that the penetration model oversimplifies the cell-nanoneedle interface.[11,22,23] The presence of nanoneedles may promote the uptake of biomolecules through a dynamic biochemical and biomechanical regulation of cell membranes.[11,24–27] A recent study also highlights that nanoneedles can even regulate the expression of nuclear genes via mechanotransduction.[28] Taken together, these findings indicate the need for in-depth investigations of the cell-nanoneedle interface.

We recently introduced electrodeposited electrodes for studying the interaction between cells and nanostructures.[29,30] Our electrodeposition method is highly tunable to the fabrication of microarchitectures with different degrees of nanostructuring in a template-mediated[31–33] or template-free manner.[34] Notably, nanoneedles with highly tunable geometries and densities can be deposited onto the bare gold surface in a few minutes with a simple setup.[34] This motivated us to adapt electrodeposition as a means for rapid, RIE-free fabrication of nanoneedles.

Here, we report the first use of electrodeposition to fabricate gold nanoneedles for intracellular delivery in hard-to-transfect primary and stem cells. Our electrodeposition method is rapid, RIE-free, scalable, and relatively low-cost. We investigated the relationship between nanoneedle morphology, delivery efficiency, and cytotoxicity. We found the gold nanoneedles with different morphology had minimal effects on the viability and apoptosis of cells based on the staining of Annexin V. Highly spiky nanoneedles deposited under the voltage of 0 mV and -300 mV resulted in better delivery efficiency. Various exogenous biomolecules (dextran, albumin, transferrin, quantum dot, siRNA) were successfully delivered with the help of electrodeposited nanoneedles into primary and stem cells, including pluripotent stem cells, mesenchymal stem cells, endothelial cells, and primary fibroblasts. We also studied the mechanism underlying the improved efficiency. It was found that the electrodeposited nanoneedles promote the endocytosis of biomolecules via arresting cells on the G2 cell cycle. Further microarrayed and mass spectrometric analysis reveals that such cell cycle arrest

originated from the limited adhesion on the cell membrane, transduced to the nucleus via the NFκB pathway, and achieved through regulating E2F and CDK proteins in the nucleus. Taken together, our findings prove the utility of electrodeposited gold nanoneedles for the generic delivery of biomolecules and provide biological insights into the interaction between complex nanostructures and sensitive primary cells beyond the current membrane disruption model. We believe this novel perspective is useful for the design of next-generation multifunctional biointerfaces.

Our nanoneedles are generated on a mask-free gold-coated glass substrate (Fig. 1A). The fabrication procedure only involves one-step electrodeposition running at direct current potential amperometry (DCPA). This one-step procedure can be performed at any benchtop potentiostat, offering great simplicity compared to other fabrication methods that typically require access to a dedicated cleanroom facility for photolithography and RIE.[2,28,35,36] Another advantage of electrodeposition is its ability to fabricate a large surface area at a time – we have validated the DCPA can be performed properly on 5-inch gold-coated glass wafers. The scalability is potentially useful when scaling up the application of nanoneedles for the large-scale manufacturing of therapeutic cells.

During DCPA, the morphogenesis of nanoneedles can be precisely controlled via tuning the potential on cathodes. Increasingly positive potential limits the nucleation of gold ion ($AuCl_4^-$) in $HAuCl_4$ solution to metallic gold.[37] As a result, the nanoneedles deposited under a higher positive potential have smaller size and spikiness of needles,[34] as revealed by the scanning electron microscopy (SEM, Fig. 1B). Hence, to favor the formation of nanoneedles, it is desired to apply zero or negative potentials to speeds up the nucleation – this yields in the creation of nanostructured microarchitectures (NMA) consisting nanoneedles on its deposition front (Fig. 1B). The diameter of deposited nanoneedles is tunable through the potential - potentials of 0 mV and -300 mV generate nanoneedles with diameters of 100 and 500 nm, respectively. It is worth noting that the electrodeposition is not able to control the orientation of NMAs and associated

nanoneedles compared to RIE-based approaches.[2,28,35,36] However, considering its high degree of nanostructuring, the NMAs still contain sufficient amounts of nanoneedles oriented upright for direct contact with the cell membranes.

Characterization of NMA biocompatibility is a prerequisite for delivery. We therefore evaluated the cytotoxicity of NMAs using an Annexin V/Dead cell staining assay by flow cytometry, where Annexin V stains apoptotic cells and NucGreen Dead dye stains necrotic cells. We assessed the viability of HES2, a human embryonic stem cell line (hESC) after 2 days' culture on NMAs with different spikiness (Fig. 1C) and observed minor changes in terms of viability and apoptosis (Fig. 1D). This demonstrates the short-term biocompatibility of NMAs and enables its use as a means for intracellular delivery. To have a better idea of the impact of NMAs on hESCs, we recultured the Day 2 cells released from the NMAs. A cocktail of SOX2/Oct4/SSEA5 was utilized to quantify the phenotypes of hESCs using flow cytometry (Fig. 1E and S1A) and fluorescent microscopy (Fig. S1B). We did not observe noticeable alternation in cell morphology and expression of pluripotent markers. This finding indicates that the NMAs are not only biocompatible but also have little impact on phenotypic variation in the short term (2 days).

We performed a series of experiments to deliver various biomolecules into hESCs. We tested delivery with Alexa Fluor 647-labeled transferrin, a glycoprotein protein that mediates the transport of iron through blood plasma. The uptake of transferrin is strictly regulated through clathrin-mediated endocytosis[38] and therefore is a good indicator of endocytotic activities. We found that the cells on NMAs experienced much higher uptake of transferrin compared to ones on flat vessels (81.9% vs 42.2%, Fig. 2A). A similar trend was also observed with quantum dots, a nanomaterial that is largely taken by clathrin-mediated endocytosis.[39] Interestingly, the delivery efficiency of sharp nanoneedles (0 mV and -300 mV) is considerably better than mild nanopits (Fig. 2B). Taken together, this suggests that the presence of NMAs, especially high aspect-ratio nanoneedles, promotes the clathrin-mediated endocytosis. Indeed, this observation is in high agreement with

a previous study reporting that the nanoneedles help the formation of clathrin-coated pits for vesicle intake.[11]

Endocytosis is a major pathway for the uptake of many common biomolecules, including dextran.[40] We next used dextran with different molecular weights to benchmark the generality of upregulated endocytosis (Fig. 2C). A global increase of uptake was observed from the molecular weight of 3kDa to 500kDa, although the uptake of 500k dextran on NMAs was still relatively low (< 30%) after 24 hours. Hence, we concluded that the presence of NMAs benefits the endocytotic intake of common biomolecules and could effectively help the delivery of biomolecules up to 70kDa. In addition, we observed little (< 20%) uptake of albumin on flat and NMA conditions, although the albumin is internalized mostly through endocytosis.[41] The mechanism behind this observation is unclear. The added albumin may interact with the soluble fibroblast growth factors (FGF) present in the hESC medium[42,43] before the cellular uptake.

We also seeded multiple different primary cells, including adipose-derived stem cells (ADSC), human umbilical vein endothelial cells (HUVEC), primary fibroblast cells (18-CO, isolated from human colon tissues), and BYS-0113 human induced pluripotent stem cells (hiPSC, Fig 2D). Upregulated intake of dextran and albumin were consistently observed, indicating that NMA-mediated upregulation of endocytosis is applicable to multiple cell types.

Common transfection reagents, such as lipofectamine, utilize endocytosis to deliver specific DNA and RNA into cells.[44] Hence, the NMA-mediated upregulation of endocytosis may also benefit the delivery of DNA and RNA. To test this, we delivered a variety of small interfering RNA (siRNA) into hESCs, hiPSCs, and ADSCs. The siRNA was fluorescently labeled by Cy5 or FAM. The transfection efficiency was quantified by flow cytometry (Fig. 3A – 3C). We observed an upregulated intake of siRNA at the RNA level. To verify the integrity and functionality of delivered siRNA, we examined the knockdown (KD) of siRNA-targeted protein at the protein level (Fig. 3D and 3F). Similar to the results at the RNA level, cells cultured on NMAs had lower expression of the target protein,

indicating a higher KD efficiency. We achieved a 75% KD of GAPDH on hESCs and 90% KD of Vimentin on ADSCs, which is comparable to the well-optimized KD protocol for stem cells.[45] It is worth noting that we achieved such efficiency with only one round of transfection in 24 hrs while the previous protocol requires multiple rounds of transfection in 72 hrs to 6 days.[45] Hence, NMA-mediated upregulation of endocytosis holds great potential for rapid and efficient DNA/RNA delivery.

Next, we sought to investigate the mechanism of the increased endocytosis. A comprehensive proteome analysis was performed based on mass spectrometry. Differential protein expression was carried out by comparing the total peptide number from each sample. Proteins were considered differentially upregulated if fold change (NMA/control) is greater than 4 (equivalent to $\log_2(FC) > 2$). Lists of upregulated proteins were submitted to Metascape[46] for over-representation analysis (Fig. 4A). Not surprisingly, membrane trafficking, cytoskeleton-dependent intracellular transportation, and organelle organization occur in the top-10 enriched pathways. This matches well with our observation of upregulated endocytotic activities. Interestingly, cell cycle and cell phase-related pathways also show up multiple times in the top 10 enriched pathways, revealing a possible alternation in cell cycle. With this in mind, we performed cell cycle analysis using flow cytometry and noticed a significant modulation (Fig. 4B and 4C). Compared to the cells seeded on a flat substrate, the one on the NMAs had a noteworthy increase in the percentage of G2/M phase. Quantitative analysis revealed a negative correlation between the potential of deposition (equivalently to the spikiness of NMAs) and the percentage of cells in the G2/M phase. Highly spiky NMAs (0 mV and -300 mV) can arrest around 60% of cells on the G2/M phase. To accurately identify the phase of arrest, we stained the samples with histone H3 pS28, a M phase-specific phosphorylated protein and confirmed less than 2% of the cells on 0 mV NMA substrate were on M phase (Fig. 4D). With this in mind, we concluded that the cells on spiky NMAs underwent significant G2 arrest.

The uptake of exogenous biomolecules is a cell-cycle-dependent process. Numerous studies have demonstrated the uptake of nanoparticles,[47] lipoplex,[48] polyplex,[48] metal compound,[49] as well as membrane permeability,[38] are strongly correlated to the cell cycle. Cells in G2 cycles have much higher delivery/transfection efficiency compared to the ones in G0/G1 cycle. For some cell lines, such difference can be up to 30 – 500 fold higher as quantified by the activity of transfected luciferase.[48] These studies support our observations that the highly spiky NMAs induced G2 arrest and such arrest benefited the delivery of exogenous biomolecules.

To identify the key regulators in this microenvironment-induced cell cycle arrest, we subsequently performed mRNA-based microarray analysis. We surveyed 48 and 96 essential genes in cell cycle regulation and cell adhesion, respectively (Fig. 4D and S2). For the cell cycle, we found the E2F family was significantly upregulated when seeding cells on NMAs. Within, expression of *E2F4* has been reported to regulate a stable G2 arrest in prostate carcinoma.[50] Most of the members in E2F family, including *E2F2* and *E2F4*, were recently identified to highly expressed in non-G0/G1 cells, indicating their roles in maintaining cells in S-G2-M phases.[51] In addition, the top downregulated gene in the cell cycle is *CDKN1B*, a promotor for G1 arrest.[52] Hence, we concluded that the NMA causes G2 arrest by upregulating E2F family and downregulating *CDKN1B* in the nucleus. For cell adhesion, we noticed that over 90% of the genes were upregulated on NMAs and the top upregulated genes are corresponding to cell-cell junction (*ICAM1*, *HAS1*). This finding is consistent with our previous observation that cells underwent limited adhesion and membrane disruption on NMA and therefore promote cell-cell adhesion to avoid anoikis.[34]

To search for the possible pathways that transduce the mechanical signaling from the membrane to the nucleus for cell cycle arrest, we performed TRRUST analysis (Transcriptional Regulatory Relationships Unraveled by Sentence-based Text mining)[53] using the list consisting of regulated genes/proteins. There are three shared genes (*SP1*, *RELA*, *NFKB1*) in the transcriptional regulators of the hits from

cell cycle and adhesion (Fig. 4F and Fig. S3) at the RNA level. *SP1* is also a shared gene when overlapping transcriptome and proteome. Indeed, *SP1* interacts with most of the top hits discussed above, such as E2F families,[54,55] *COL11A1*,[56] *ICAM1*,[57] and *HAS1*.[58] This suggests the central role of *SP1* of converting mechanical alternation into cell cycle arrest. Interestingly, *SP1*, *RELA* and *NFKB1* are all involved in the NFκB (nuclear factor kappa-light-chain-enhancer of activated B cells) pathway where *RELA* and *NFKB1* encoded two members of the NFKB protein family.[59] With this in mind, we believed NFκB pathway is very likely to mediate the NMA-induced cell cycle arrest.

We performed a dot blot of 41 proteins involved in NFκB pathway to deconvolute the mechanotransduction from membrane to nucleus. We observed a noticeable decrease (> 20% compared to flat control) of NFKB1, STAT1, STAT2, IKKγ, IL-17 RA, RELA, and MYD88 (Fig. 4G and Fig. S4). Within, the presence of NFKB1 and RELA at the protein level confirms the validity of the transcriptional analysis. Indeed, the expression and translocation of NFKB1 and RELA are directly regulated by IKKγ in NFκB pathway.[60] IKKγ, also known as NEMO, can be modulated by various stimuli from ECM, including compressive force,[61,62], and fluid shear.[63,64] For example, dynamic tensile strain has shown a negative impact on IKKγ expression in human chondrocytes.[61]

With the data from transcriptome and proteome in mind, we proposed a schematic of the mechanism of NMA-mediated cell cycle arrest and upregulated endocytotic activities (Fig. 4H). The inadequate surface on the sharp needle of NMA forces seeded cells to undergo limited adhesion, upregulated cell-cell adhesion, and introduced mechanical strain stress. Such stress was sensed by IKKγ and transduced via RelA and NFκB to the nucleus. RelA and NFκB react with SP1 in the nucleus, promoted the expression of E2F families, downregulated the expression of *CDKN1B*. Such alteration pushed cells to depart from the G1 phase and be arrested at the G2 phase, which favors the endocytosis of exogenous biomolecules.

In summary, we developed a rapid, RIE-free protocol to fabricate nanostructured microarchitectures (NMA) with tunable nanostructuring via electrodeposition. NMAs were found to significantly promote the endocytosis of proteins and siRNA in primary cells, which improves the efficiency of gene knockdown. We performed a comprehensive analysis of transcriptome and proteome to reveal the underlying mechanism. We concluded that endocytosis is a result of cell cycle arrest transduced from NMAs to nucleus through the NF-κB pathway. Taken together, our results demonstrate that the presence of high-aspect-ratio nanostructures in biointerfaces can induce more complex biological responses than membrane deformation. The interaction with nanostructures will alter multiple intracellular processes, such as signaling transduction and cell cycle. Importantly, the nanostructure-induced cell cycle arrest can be utilized to improve the cellular endocytic process and yield efficient intracellular delivery. It will be useful to consider the features characterized when designing the future multifunctional biointerfaces to further heighten the efficiency of drug delivery strategies.

EXPERIMENTAL SECTIONS

The experimental sections are included in the supporting information.

SUPPORTING INFORMATION

Supporting Information (SI) is available from free of charge on the website. The SI contains experimental sections, details of antibodies, and additional data characterizing the cellular behavior on nanostructured microarchitectures.

CONFLICT OF INTEREST

The authors declare no conflict of interest.

AUTHOR CONTRIBUTIONS

Z. W and S.O.K conceived and designed the experiments. Z. W, H. W, S. L, M. L performed the experiments and analyzed the data. All authors discussed the results and contributed to the preparation and editing of the manuscript.

ACKNOWLEDGEMENTS

This research was supported in part by the Canadian Institutes of Health Research (grant no. FDN-148415), the Natural Sciences and Engineering Research Council of Canada (grant no. RGPIN-2016-06090). This research is part of the University of Toronto's Medicine by Design initiative, which receives funding from the Canada First Research Excellence Fund. Z.W. was supported by an Alexander Graham Bell Canada Graduate Scholarship and a Centre for Pharmaceutical Oncology Graduate Student Scholarship.

REFERENCES

(1) Stewart, M. P.; Sharei, A.; Ding, X.; Sahay, G.; Langer, R.; Jensen, K. F. In Vitro and Ex Vivo Strategies for Intracellular Delivery. *Nature* **2016**, *538* (7624), 183–192. https://doi.org/10.1038/nature19764.

(2) Xu, X.; Hou, S.; Wattanatorn, N.; Wang, F.; Yang, Q.; Zhao, C.; Yu, X.; Tseng, H. R.; Jonas, S. J.; Weiss, P. S. Precision-Guided Nanospears for Targeted and High-Throughput Intracellular Gene Delivery. *ACS Nano* **2018**, *12* (5), 4503–4511. https://doi.org/10.1021/acsnano.8b00763.

(3) Shi, H.; Xue, T.; Yang, Y.; Jiang, C.; Huang, S.; Yang, Q.; Lei, D.; You, Z.; Jin, T.; Wu, F.; Zhao, Q.; Ye, X. Microneedle-Mediated Gene Delivery for the Treatment of Ischemic Myocardial Disease. *Sci. Adv.* **2020**, *6* (25), eaaz3621. https://doi.org/10.1126/sciadv.aaz3621.

(4) Dul, M.; Stefanidou, M.; Porta, P.; Serve, J.; O'Mahony, C.; Malissen, B.; Henri, S.; Levin, Y.; Kochba, E.; Wong, F.; Dayan, C.; Coulman, S.; Birchall, J. Hydrodynamic Gene Delivery in Human Skin Using a Hollow Microneedle Device. *Journal of Controlled Release* **2017**, *265*, 120–131. https://doi.org/10.1016/j.jconrel.2017.02.028.

(5) Qu, M.; Kim, H.-J.; Zhou, X.; Wang, C.; Jiang, X.; Zhu, J.; Xue, Y.; Tebon, P.; Sarabi, S. A.; Ahadian, S.; Dokmeci, M. R.; Zhu, S.; Gu, Z.; Sun, W.; Khademhosseini, A. Biodegradable Microneedle Patch for Transdermal Gene Delivery. *Nanoscale* **2020**, *12* (32), 16724–16729. https://doi.org/10.1039/D0NR02759F.

(6) Choi, S.-O.; Kim, Y.-C.; Lee, J. W.; Park, J.-H.; Prausnitz, M. R.; Allen, M. G. Intracellular Protein Delivery and Gene Transfection by Electroporation Using a Microneedle Electrode Array. *Small* **2012**, *8* (7), 1081–1091. https://doi.org/10.1002/smll.201101747.

(7) Higgins, S. G.; Becce, M.; Belessiotis-Richards, A.; Seong, H.; Sero, J. E.; Stevens, M. M. High-Aspect-Ratio Nanostructured Surfaces as Biological Metamaterials. *Advanced Materials* **2020**, *32* (9), 1–44. https://doi.org/10.1002/adma.201903862.

(8) Choi, M.; Lee, S. H.; Kim, W. B.; Gujrati, V.; Kim, D.; Lee, J.; Kim, J. Il; Kim, H.; Saw, P. E.; Jon, S. Intracellular Delivery of Bioactive Cargos to Hard-to-Transfect Cells Using Carbon Nanosyringe Arrays under an Applied Centrifugal g-Force. *Advanced Healthcare Materials* **2016**, *5* (1), 101–107. https://doi.org/10.1002/adhm.201400834.

(9) Chiappini, C.; Martinez, J. O.; De Rosa, E.; Almeida, C. S.; Tasciotti, E.; Stevens, M. M. Biodegradable Nanoneedles for Localized Delivery of Nanoparticles in Vivo: Exploring the Biointerface. *ACS Nano* **2015**, *9* (5), 5500–5509. https://doi.org/10.1021/acsnano.5b01490.

(10) Chen, X.; Zhu, G.; Yang, Y.; Wang, B.; Yan, L.; Zhang, K. Y.; Lo, K. K. W.; Zhang, W. A Diamond Nanoneedle Array for Potential High-Throughput Intracellular Delivery. *Advanced Healthcare Materials* **2013**, *2* (8), 1103–1107. https://doi.org/10.1002/adhm.201200362.
(11) Gopal, S.; Chiappini, C.; Penders, J.; Leonardo, V.; Seong, H.; Rothery, S.; Korchev, Y.; Shevchuk, A.; Stevens, M. M. Porous Silicon Nanoneedles Modulate Endocytosis to Deliver Biological Payloads. *Advanced Materials* **2019**, *31* (12), 1806788. https://doi.org/10.1002/adma.201806788.
(12) Xu, A. M.; Wang, D. S.; Shieh, P.; Cao, Y.; Melosh, N. A. Direct Intracellular Delivery of Cell-Impermeable Probes of Protein Glycosylation by Using Nanostraws. *ChemBioChem* **2017**, *18* (7), 623–628. https://doi.org/10.1002/cbic.201600689.
(13) Chiappini, C.; De Rosa, E.; Martinez, J. O.; Liu, X.; Steele, J.; Stevens, M. M.; Tasciotti, E. Biodegradable Silicon Nanoneedles Delivering Nucleic Acids Intracellularly Induce Localized in Vivo Neovascularization. *Nature Materials* **2015**, *14* (5), 532–539. https://doi.org/10.1038/nmat4249.
(14) Wang, C.; Ye, Y.; Hochu, G. M.; Sadeghifar, H.; Gu, Z. Enhanced Cancer Immunotherapy by Microneedle Patch-Assisted Delivery of Anti-PD1 Antibody. *Nano Letters* **2016**, *16* (4), 2334–2340. https://doi.org/10.1021/acs.nanolett.5b05030.
(15) Park, S.; Choi, S. O.; Paik, S. joon; Choi, S.; Allen, M.; Prausnitz, M. Intracellular Delivery of Molecules Using Microfabricated Nanoneedle Arrays. *Biomedical Microdevices* **2016**, *18* (1), 1–13. https://doi.org/10.1007/s10544-016-0038-2.
(16) Cao, Y.; Ma, E.; Cestellos-Blanco, S.; Zhang, B.; Qiu, R.; Su, Y.; Doudna, J. A.; Yang, P. Nontoxic Nanopore Electroporation for Effective Intracellular Delivery of Biological Macromolecules. *Proceedings of the National Academy of Sciences of the United States of America* **2019**, *116* (16), 7899–7904. https://doi.org/10.1073/pnas.1818553116.
(17) Man, T.; Zhu, X.; Chow, Y. T.; Dawson, E. R.; Wen, X.; Patananan, A. N.; Liu, T. L.; Zhao, C.; Wu, C.; Hong, J. S.; Chung, P. S.; Clemens, D. L.; Lee, B. Y.; Weiss, P. S.; Teitell, M. A.; Chiou, P. Y. Intracellular Photothermal Delivery for Suspension Cells Using Sharp Nanoscale Tips in Microwells. *ACS Nano* **2019**, *13* (9), 10835–10844. https://doi.org/10.1021/acsnano.9b06025.
(18) Liu, Z.; Nie, J.; Miao, B.; Li, J.; Cui, Y.; Wang, S.; Zhang, X.; Zhao, G.; Deng, Y.; Wu, Y.; Li, Z.; Li, L.; Wang, Z. L. Self-Powered Intracellular Drug Delivery by a Biomechanical Energy-Driven Triboelectric Nanogenerator. *Advanced Materials* **2019**, *31* (12), 1–8. https://doi.org/10.1002/adma.201807795.
(19) Ding, X.; Stewart, M. P.; Sharei, A.; Weaver, J. C.; Langer, R. S.; Jensen, K. F. High-Throughput Nuclear Delivery and Rapid Expression of DNA via Mechanical and Electrical Cell-Membrane Disruption. *Nature Biomedical Engineering* **2017**, *1* (3), 1–7. https://doi.org/10.1038/s41551-017-0039.
(20) Almquist, B. D.; Melosh, N. A. Molecular Structure Influences the Stability of Membrane Penetrating Biointerfaces. *Nano Letters* **2011**, *11* (5), 2066–2070. https://doi.org/10.1021/nl200542m.
(21) Obataya, I.; Nakamura, C.; Han, S.; Nakamura, N.; Miyake, J. Nanoscale Operation of a Living Cell Using an Atomic Force Microscope with a Nanoneedle. *Nano Letters* **2005**, *5* (1), 27–30. https://doi.org/10.1021/nl0485399.
(22) Berthing, T.; Bonde, S.; Rostgaard, K. R.; Madsen, M. H.; Sørensen, C. B.; Nygård, J.; Martinez, K. L. Cell Membrane Conformation at Vertical Nanowire Array Interface Revealed by Fluorescence Imaging. *Nanotechnology* **2012**, *23* (41), 415102. https://doi.org/10.1088/0957-4484/23/41/415102.

(23) Dipalo, M.; McGuire, A. F.; Lou, H. Y.; Caprettini, V.; Melle, G.; Bruno, G.; Lubrano, C.; Matino, L.; Li, X.; De Angelis, F.; Cui, B.; Santoro, F. Cells Adhering to 3D Vertical Nanostructures: Cell Membrane Reshaping without Stable Internalization. *Nano Letters* **2018**, *18* (9), 6100–6105. https://doi.org/10.1021/acs.nanolett.8b03163.
(24) Jarsch, I. K.; Daste, F.; Gallop, J. L. Membrane Curvature in Cell Biology: An Integration of Molecular Mechanisms. *Journal of Cell Biology* **2016**, *214* (4), 375–387. https://doi.org/10.1083/jcb.201604003.
(25) Moerke, C.; Mueller, P.; Nebe, B. Attempted Caveolae-Mediated Phagocytosis of Surface-Fixed Micro-Pillars by Human Osteoblasts. *Biomaterials* **2016**, *76*, 102–114. https://doi.org/10.1016/j.biomaterials.2015.10.030.
(26) Moerke, C.; Mueller, P.; Nebe, J. B. Sensing of Micropillars by Osteoblasts Involves Complex Intracellular Signaling. *Journal of Materials Science: Materials in Medicine* **2017**, *28* (11). https://doi.org/10.1007/s10856-017-5982-8.
(27) Zhao, W.; Hanson, L.; Lou, H. Y.; Akamatsu, M.; Chowdary, P. D.; Santoro, F.; Marks, J. R.; Grassart, A.; Drubin, D. G.; Cui, Y.; Cui, B. Nanoscale Manipulation of Membrane Curvature for Probing Endocytosis in Live Cells. *Nature Nanotechnology* **2017**, *12* (8), 750–756. https://doi.org/10.1038/nnano.2017.98.
(28) Seong, H.; Higgins, S. G.; Penders, J.; Armstrong, J. P. K.; Crowder, S. W.; Moore, A. C.; Sero, J. E.; Becce, M.; Stevens, M. M. Size-Tunable Nanoneedle Arrays for Influencing Stem Cell Morphology, Gene Expression, and Nuclear Membrane Curvature. *ACS Nano* **2020**, *14* (5), 5371–5381. https://doi.org/10.1021/acsnano.9b08689.
(29) Poudineh, M.; Wang, Z.; Labib, M.; Ahmadi, M.; Zhang, L.; Das, J.; Ahmed, S.; Angers, S.; Kelley, S. O. Three-Dimensional Nanostructured Architectures Enable Efficient Neural Differentiation of Mesenchymal Stem Cells via Mechanotransduction. *Nano Letters* **2018**, *18* (11), 7188–7193. https://doi.org/10.1021/acs.nanolett.8b03313.
(30) Wang, Z.; Zhang, L.; Labib, M.; Chen, H.; Wei, M.; Poudineh, M.; Green, B. J.; Duong, B.; Das, J.; Ahmed, S.; Sargent, E. H.; Kelley, S. O. Peptide-Functionalized Nanostructured Microarchitectures Enable Rapid Mechanotransductive Differentiation. *ACS Applied Materials and Interfaces* **2019**, *11* (44), 41030–41037. https://doi.org/10.1021/acsami.9b13694.
(31) Soleymani, L.; Fang, Z.; Sargent, E. H.; Kelley, S. O. Programming the Detection Limits of Biosensors through Controlled Nanostructuring. *Nature Nanotechnology* **2009**, *4* (12), 844–848. https://doi.org/10.1038/nnano.2009.276.
(32) Lam, B.; Das, J.; Holmes, R. D.; Live, L.; Sage, A.; Sargent, E. H.; Kelley, S. O. Solution-Based Circuits Enable Rapid and Multiplexed Pathogen Detection. *Nature Communications* **2013**, *4* (May). https://doi.org/10.1038/ncomms3001.
(33) Sage, A. T.; Mahmoudian, L.; Kelley, S. O.; Besant, J. D.; Poudineh, M.; Sargent, E. H.; Bai, X.; Zamel, R.; Hsin, M.; Cypel, M.; Liu, M.; Keshavjee, S. Fractal Circuit Sensors Enable Rapid Quantification of Biomarkers for Donor Lung Assessment for Transplantation. *Science Advances* **2015**, *1* (7), 1–10. https://doi.org/10.1126/sciadv.1500417.
(34) Wang, Z.; Xia, F.; Labib, M.; Ahmadi, M.; Chen, H.; Das, J.; Ahmed, S. U.; Angers, S.; Sargent, E. H.; Kelley, S. O. Nanostructured Architectures Promote the Mesenchymal-Epithelial Transition for Invasive Cells. *ACS Nano* **2020**, *14* (5), 5324–5336. https://doi.org/10.1021/acsnano.9b07350.
(35) Kim, H.; Jang, H.; Kim, B.; Kim, M. K.; Wie, D. S.; Lee, H. S.; Kim, D. R.; Lee, C. H. Flexible Elastomer Patch with Vertical Silicon Nanoneedles for Intracellular and

Intratissue Nanoinjection of Biomolecules. *Sci. Adv.* **2018**, *4* (11), eaau6972. https://doi.org/10.1126/sciadv.aau6972.

(36) Chiappini, C.; Chen, Y.; Aslanoglou, S.; Mariano, A.; Mollo, V.; Mu, H.; De Rosa, E.; He, G.; Tasciotti, E.; Xie, X.; Santoro, F.; Zhao, W.; Voelcker, N. H.; Elnathan, R. Tutorial: Using Nanoneedles for Intracellular Delivery. *Nat Protoc* **2021**, *16* (10), 4539–4563. https://doi.org/10.1038/s41596-021-00600-7.

(37) Mahshid, S.; Mepham, A. H.; Mahshid, S. S.; Burgess, I. B.; Saberi Safaei, T.; Sargent, E. H.; Kelley, S. O. Mechanistic Control of the Growth of Three-Dimensional Gold Sensors. *J. Phys. Chem. C* **2016**, *120* (37), 21123–21132. https://doi.org/10.1021/acs.jpcc.6b05158.

(38) Mayle, K. M.; Le, A. M.; Kamei, D. T. The Intracellular Trafficking Pathway of Transferrin. *Biochimica et Biophysica Acta - General Subjects* **2012**, *1820* (3), 264–281. https://doi.org/10.1016/j.bbagen.2011.09.009.

(39) Anas, A.; Okuda, T.; Kawashima, N.; Nakayama, K.; Itoh, T.; Ishikawa, M.; Biju, V. Clathrin-Mediated Endocytosis of Quantum Dot-Peptide Conjugates in Living Cells. *ACS Nano* **2009**, *3* (8), 2419–2429. https://doi.org/10.1021/nn900663r.

(40) Li, L.; Wan, T.; Wan, M.; Liu, B.; Cheng, R.; Zhang, R. The Effect of the Size of Fluorescent Dextran on Its Endocytic Pathway. *Cell Biology International* **2015**, *39* (5), 531–539. https://doi.org/10.1002/cbin.10424.

(41) Razzak, M. Albumin Endocytosis Is Caveolin-Mediated. *Nat Rev Nephrol* **2014**, *10* (5), 242–242. https://doi.org/10.1038/nrneph.2014.47.

(42) She, Z.; Wang, C.; Li, J.; Sukhorukov, G. B.; Antipina, M. N. Encapsulation of Basic Fibroblast Growth Factor by Polyelectrolyte Multilayer Microcapsules and Its Controlled Release for Enhancing Cell Proliferation. *Biomacromolecules* **2012**, *13* (7), 2174–2180. https://doi.org/10.1021/bm3005879.

(43) Almendro, V.; Ametller, E.; García-Recio, S.; Collazo, O.; Casas, I.; Augé, J. M.; Maurel, J.; Gascón, P. The Role of MMP7 and Its Cross-Talk with the FAS/FASL System during the Acquisition of Chemoresistance to Oxaliplatin. *PLoS ONE* **2009**, *4* (3), e4728. https://doi.org/10.1371/journal.pone.0004728.

(44) Cardarelli, F.; Digiacomo, L.; Marchini, C.; Amici, A.; Salomone, F.; Fiume, G.; Rossetta, A.; Gratton, E.; Pozzi, D.; Caracciolo, G. The Intracellular Trafficking Mechanism of Lipofectamine-Based Transfection Reagents and Its Implication for Gene Delivery. *Scientific Reports* **2016**, *6* (April), 1–8. https://doi.org/10.1038/srep25879.

(45) Ma, Y.; Jin, J.; Dong, C.; Cheng, E. C.; Lin, H.; Huang, Y.; Qiu, C. High-Efficiency SiRNA-Based Gene Knockdown in Human Embryonic Stem Cells. *Rna* **2010**, *16* (12), 2564–2569. https://doi.org/10.1261/rna.2350710.

(46) Zhou, Y.; Zhou, B.; Pache, L.; Chang, M.; Khodabakhshi, A. H.; Tanaseichuk, O.; Benner, C.; Chanda, S. K. Metascape Provides a Biologist-Oriented Resource for the Analysis of Systems-Level Datasets. *Nature Communications* **2019**, *10* (1). https://doi.org/10.1038/s41467-019-09234-6.

(47) Kim, J. A.; Aberg, C.; Salvati, A.; Dawson, K. A. Role of Cell Cycle on the Cellular Uptake and Dilution of Nanoparticles in a Cell Population. *Nature Nanotechnology* **2012**, *7* (1), 62–68. https://doi.org/10.1038/nnano.2011.191.

(48) Brunner, S.; Sauer, T.; Carotta, S.; Cotten, M.; Saltik, M.; Wagner, E. Cell Cycle Dependence of Gene Transfer by Lipoplex Polyplex and Recombinant Adenovirus. *Gene Therapy* **2000**, *7* (5), 401–407. https://doi.org/10.1038/sj.gt.3301102.

(49) Yoshida, F.; Matsumura, A.; Shibata, Y.; Yamamoto, T.; Nakauchi, H.; Okumura, M.; Nose, T. Cell Cycle Dependence of Boron Uptake from Two Boron Compounds Used for Clinical Neutron Capture Therapy. *Cancer Letters* **2002**, *187* (1–2), 135–141. https://doi.org/10.1016/S0304-3835(02)00380-4.

(50) Crosby, M. E.; Jacobberger, J.; Gupta, D.; Macklis, R. M.; Almasan, A. E2F4 Regulates a Stable G2 Arrest Response to Genotoxic Stress in Prostate Carcinoma. *Oncogene* **2007**, *26* (13), 1897–1909. https://doi.org/10.1038/sj.onc.1209998.
(51) Cuitiño, M. C.; Pécot, T.; Sun, D.; Kladney, R.; Okano-Uchida, T.; Shinde, N.; Saeed, R.; Perez-Castro, A. J.; Webb, A.; Liu, T.; Bae, S. I.; Clijsters, L.; Selner, N.; Coppola, V.; Timmers, C.; Ostrowski, M. C.; Pagano, M.; Leone, G. Two Distinct E2F Transcriptional Modules Drive Cell Cycles and Differentiation. *Cell Reports* **2019**, *27* (12), 3547-3560.e5. https://doi.org/10.1016/j.celrep.2019.05.004.
(52) Satoh, T.; Kaida, D. Upregulation of P27 Cyclin-Dependent Kinase Inhibitor and a C-Terminus Truncated Form of P27 Contributes to G1 Phase Arrest. *Scientific Reports* **2016**, *6* (May), 1–8. https://doi.org/10.1038/srep27829.
(53) Han, H.; Cho, J. W.; Lee, S.; Yun, A.; Kim, H.; Bae, D.; Yang, S.; Kim, C. Y.; Lee, M.; Kim, E.; Lee, S.; Kang, B.; Jeong, D.; Kim, Y.; Jeon, H. N.; Jung, H.; Nam, S.; Chung, M.; Kim, J. H.; Lee, I. TRRUST v2: An Expanded Reference Database of Human and Mouse Transcriptional Regulatory Interactions. *Nucleic Acids Research* **2018**, *46* (D1), D380–D386. https://doi.org/10.1093/nar/gkx1013.
(54) Karlseder, J.; Rotheneder, H.; Wintersberger, E. Interaction of Sp1 with the Growth- and Cell Cycle-Regulated Transcription Factor E2F. *Molecular and Cellular Biology* **1996**, *16* (4), 1659–1667. https://doi.org/10.1128/mcb.16.4.1659.
(55) Rotheneder, H.; Geymayer, S.; Haidweger, E. Transcription Factors of the Sp1 Family: Interaction with E2F and Regulation of the Murine Thymidine Kinase Promoter. *Journal of Molecular Biology* **1999**, *293* (5), 1005–1015. https://doi.org/10.1006/jmbi.1999.3213.
(56) Watanabe, K.; Hida, M.; Sasaki, T.; Yano, H.; Kawano, K.; Yoshioka, H.; Matsuo, N. Sp1 Upregulates the Proximal Promoter Activity of the Mouse Collagen A1(XI) Gene (Col11a1) in Chondrocytes. *In Vitro Cellular and Developmental Biology - Animal* **2016**, *52* (2), 235–242. https://doi.org/10.1007/s11626-015-9959-y.
(57) Koizume, S.; Ito, S.; Nakamura, Y.; Yoshihara, M.; Furuya, M.; Yamada, R.; Miyagi, E.; Hirahara, F.; Takano, Y.; Miyagi, Y. Lipid Starvation and Hypoxia Synergistically Activate ICAM1 and Multiple Genes in an Sp1-Dependent Manner to Promote the Growth of Ovarian Cancer. *Molecular Cancer* **2015**, *14* (1), 2–3. https://doi.org/10.1186/s12943-015-0351-z.
(58) Monslow, J.; Williams, J. D.; Fraser, D. J.; Michael, D. R.; Foka, P.; Kift-Morgan, A. P.; Dong, D. L.; Fielding, C. A.; Craig, K. J.; Topley, N.; Jones, S. A.; Ramji, D. P.; Bowen, T. Sp1 and Sp3 Mediate Constitutive Transcription of the Human Hyaluronan Synthase 2 Gene. *Journal of Biological Chemistry* **2006**, *281* (26), 18043–18050. https://doi.org/10.1074/jbc.M510467200.
(59) Nabel, G. J.; Verma, I. M. Proposed NF-KB/IκB Family Nomenclature. *Genes and Development* **1993**, *7* (11), 2063. https://doi.org/10.1101/gad.7.11.2063.
(60) Perkins, N. D. Integrating Cell-Signalling Pathways with NF-KB and IKK Function. *Nature Reviews Molecular Cell Biology* **2007**, *8* (1), 49–62. https://doi.org/10.1038/nrm2083.
(61) Anghelina, M.; Sjostrom, D.; Perera, P.; Nam, J.; Knobloch, T.; Agarwal, S. Regulation of Biomechanical Signals by NF-KappaB Transcription Factors in Chondrocytes. *Biorheology* **2008**, *45* (3–4), 245–256. https://doi.org/10.1016/j.physbeh.2017.03.040.
(62) Nam, J.; Aguda, B. D.; Rath, B.; Agarwal, S. Biomechanical Thresholds Regulate Inflammation through the NF-KB Pathway: Experiments and Modeling. *PLoS ONE* **2009**, *4* (4). https://doi.org/10.1371/journal.pone.0005262.
(63) Khachigian, L. M.; Resnick, N.; Gimbrone, M. A.; Collins, T. Nuclear Factor-KB Interacts Functionally with the Platelet-Derived Growth Factor B-Chain Shear-

Stress Response Element in Vascular Endothelial Cells Exposed to Fluid Shear Stress. *Journal of Clinical Investigation* **1995**, *96* (2), 1169–1175. https://doi.org/10.1172/JCI118106.

(64) Chen, N. X.; Geist, D. J.; Genetos, D. C.; Pavalko, F. M.; Duncan, R. L. Fluid Shear-Induced NFκB Translocation in Osteoblasts Is Mediated by Intracellular Calcium Release. *Bone* **2003**, *33* (3), 399–410. https://doi.org/10.1016/S8756-3282(03)00159-5.

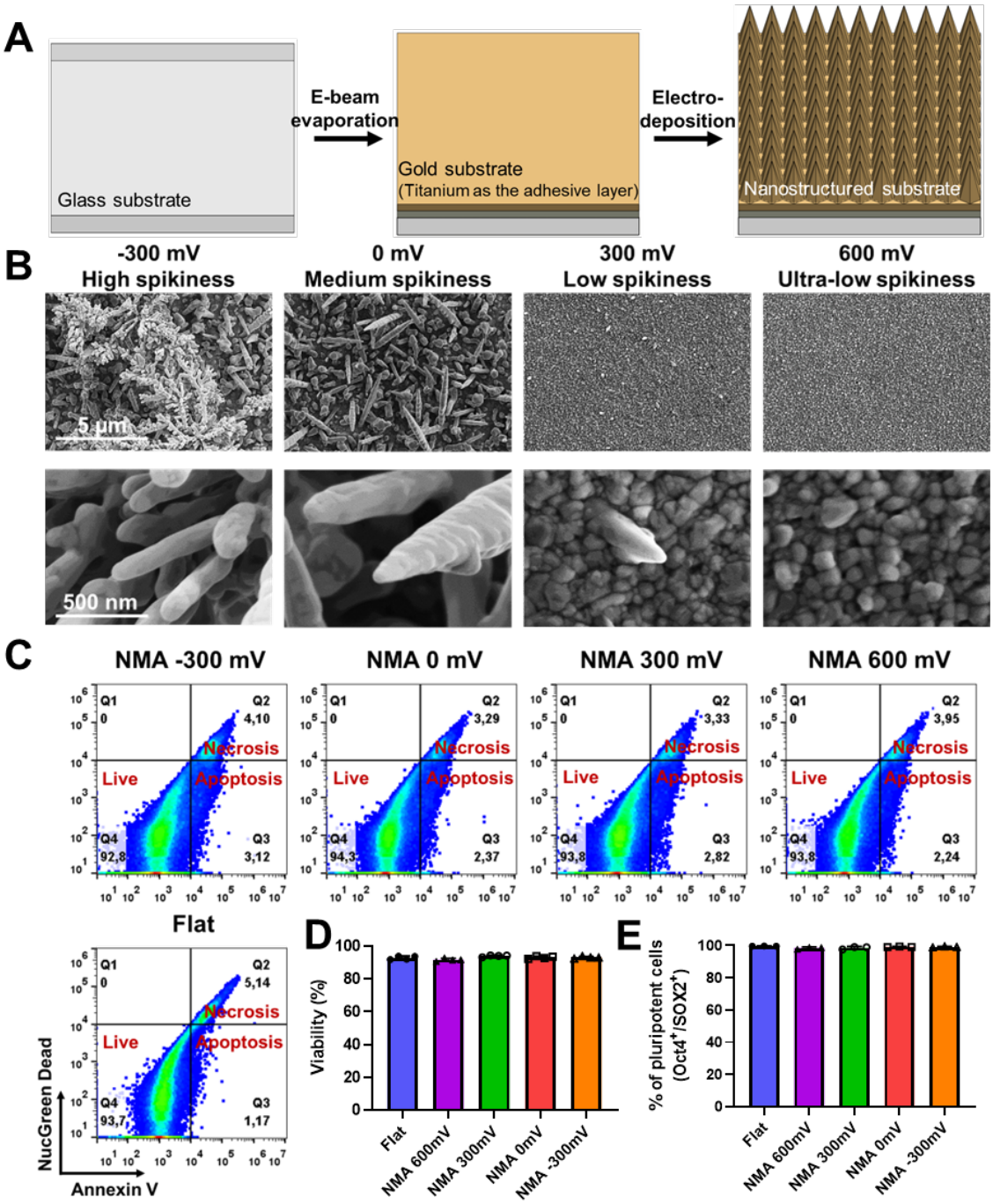

Figure 1. Electrodeposition of biocompatible nanostructured microarchitectures (NMAs) with tunable morphology and density of nanoneedles. (A) One-step fabrication of NMAs via electrodeposition. (B) Morphology of NMAs deposited under different potentials. (C) Representative flow cytometric profile showing the percentage of live, apoptotic and necrotic cells recovered from NMAs. (D) Quantitation of cell viability. (E) Quantitation of pluripotency.

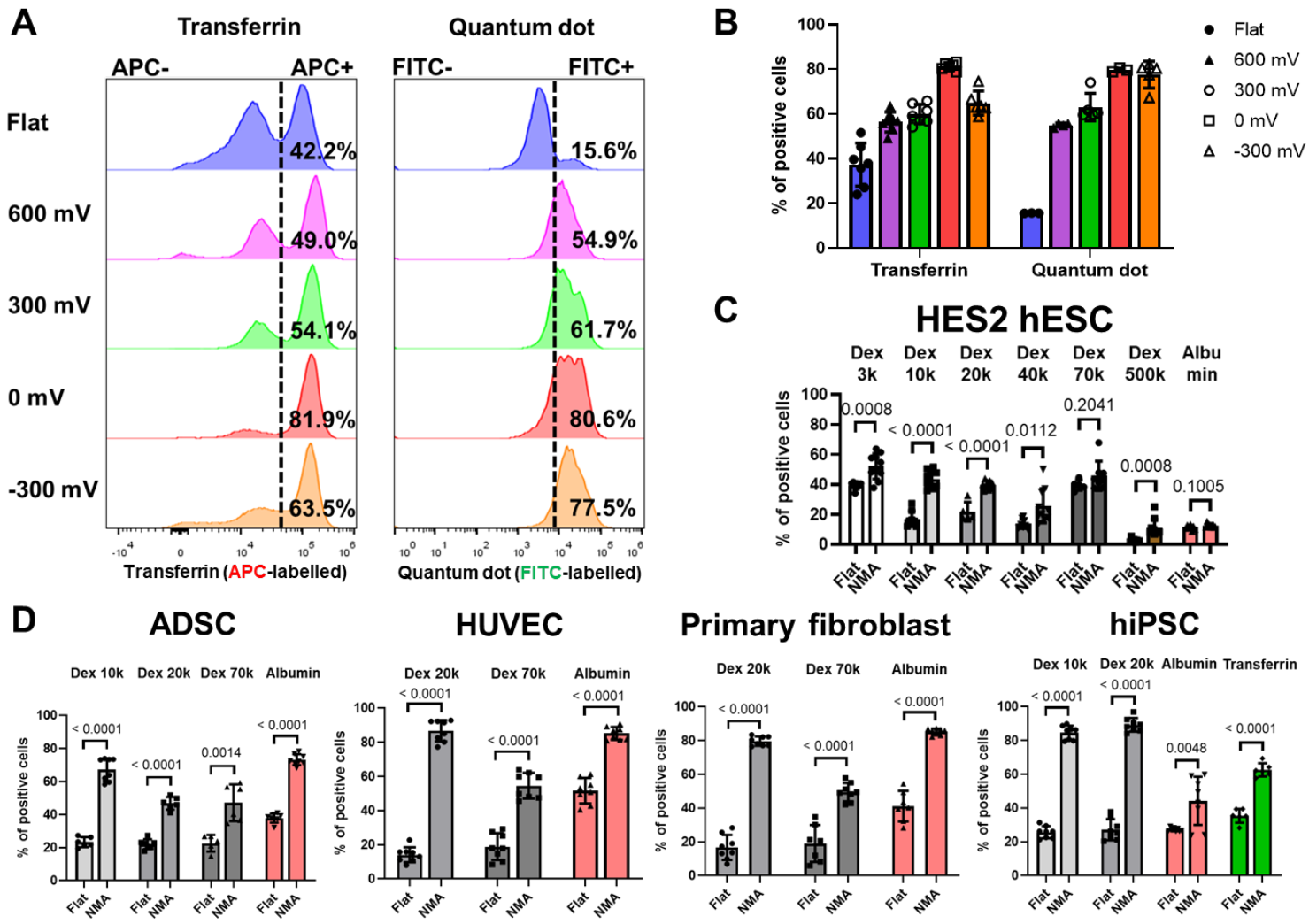

Figure 2. NMAs containing high-density nanoneedles promote the delivery of various biological molecules across multiple hard-to-transfect primary cells. (A) Representative flow cytometric profile of HES2 embryonic stem cells treated with fluorescently labeled transferrin for 6 hrs and quantum dots (QD) for 24 hrs. (B) Quantitation of deliver efficiency on different substrates. (C) Quantitation of deliver efficiency of dextran cargos on HES2 cells after 6 hrs. (D) Quantitation of deliver efficiency of NMA 0mV substrates for multiple primary cells after 24 hrs. Each dot represents a technical replicate. At least 3 biological replicates for each group.

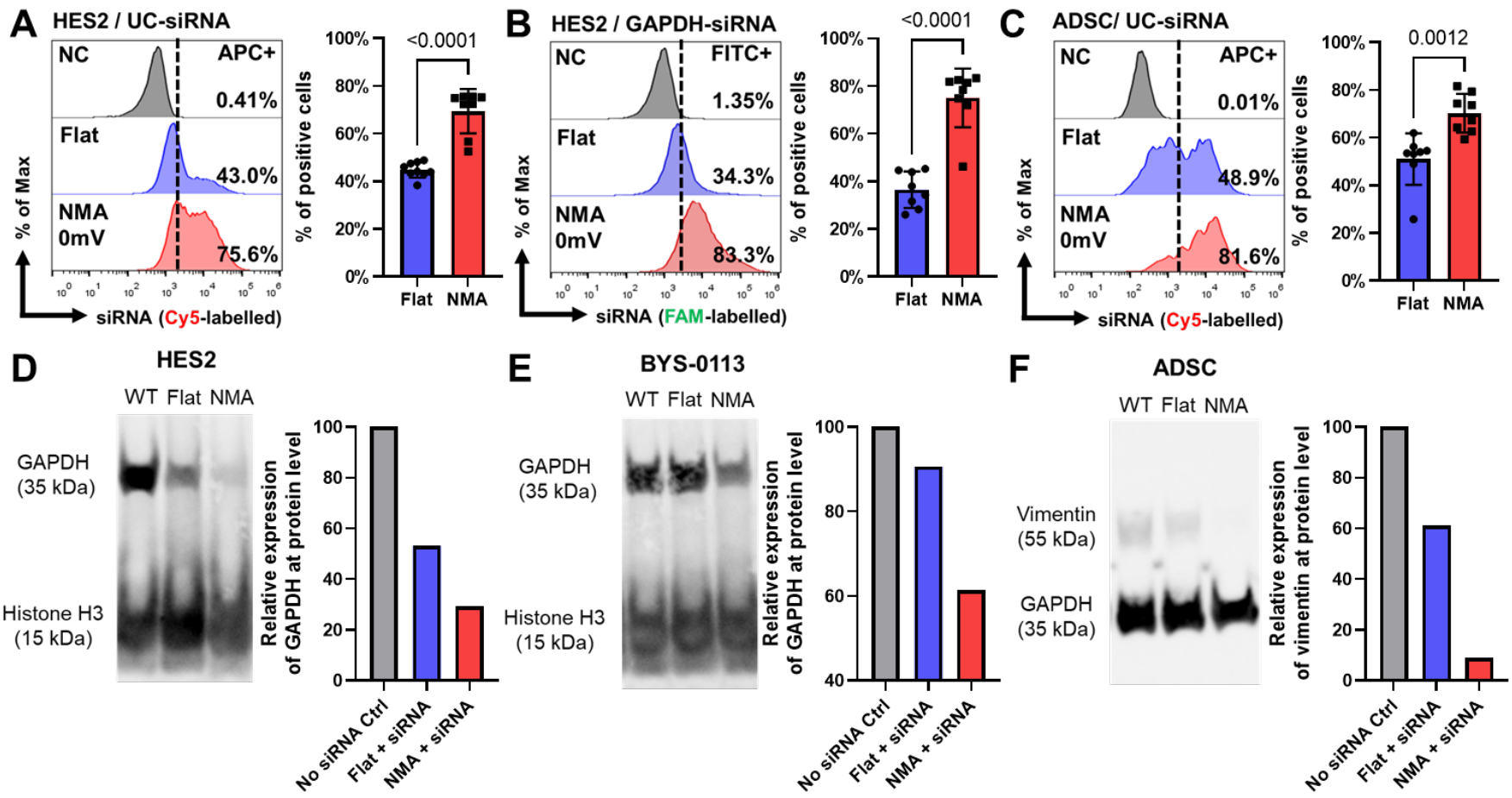

Figure 3. NMAs containing high-density nanoneedles promote the lipofection of siRNA and yield significant knockdown at the protein level. (A-C) Representative flow cytometric profile of HES2 embryonic stem cells (A-B) and adipose-derived stem cells (ADSC) treated with fluorescently labeled siRNA for 6 hrs. (D-E) Quantitation of the GAPDH expression on HES2 and BYS-0113 cells 60 hours post-lipofection. (F) Quantitation of the Vimentin expression on ADSC cells 60 hours post-lipofection.

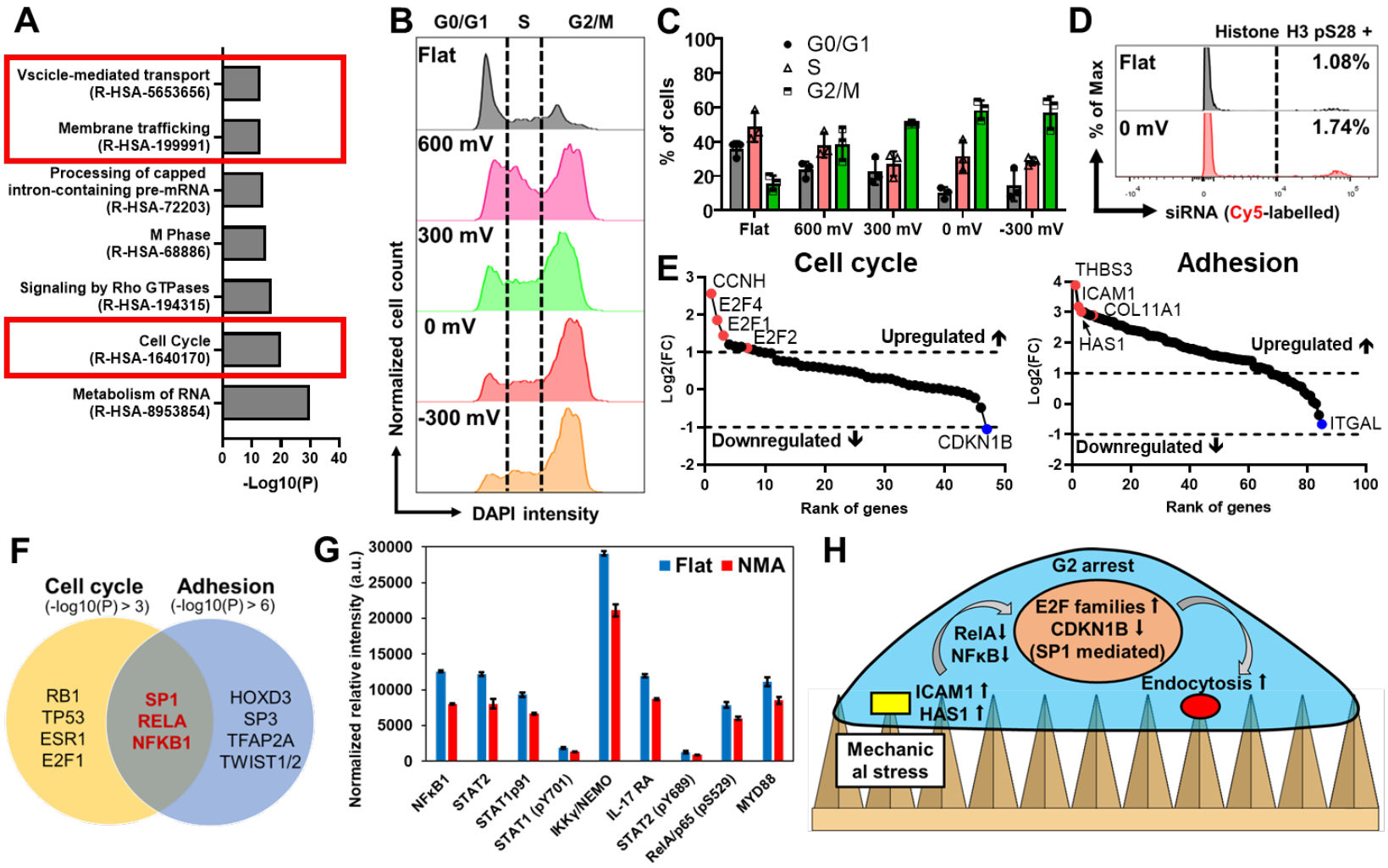

Figure 4. NMAs promotes membrane traffic via cell cycle arrest. (A) Top enriched pathways from label-free mass spectrometry analysis. (B) Flow cytometric analysis of the cell cycle of cells seeded on the NMAs. (C) Quantitation of the percentage of cells in each cell cycle. (D) Flow cytometric analysis of the expression of histone H3 pS28, a mitosis-specific biomarker. (E) Differentially expressed genes in the process of cell cycle and cellular adhesion revealed by Taqman qPCR array. (F) Results of TRRUST analysis revealing the NFKB-related TFs play a key role in the signal transduction. (G) Dot plot results regarding the major proteins involved in the NFKB pathways. The error bar indicates standard deviation from duplicates. (H) Proposed mechanism of signaling transduction for NMA-mediated cell cycle arreast and endocytosis promotion.

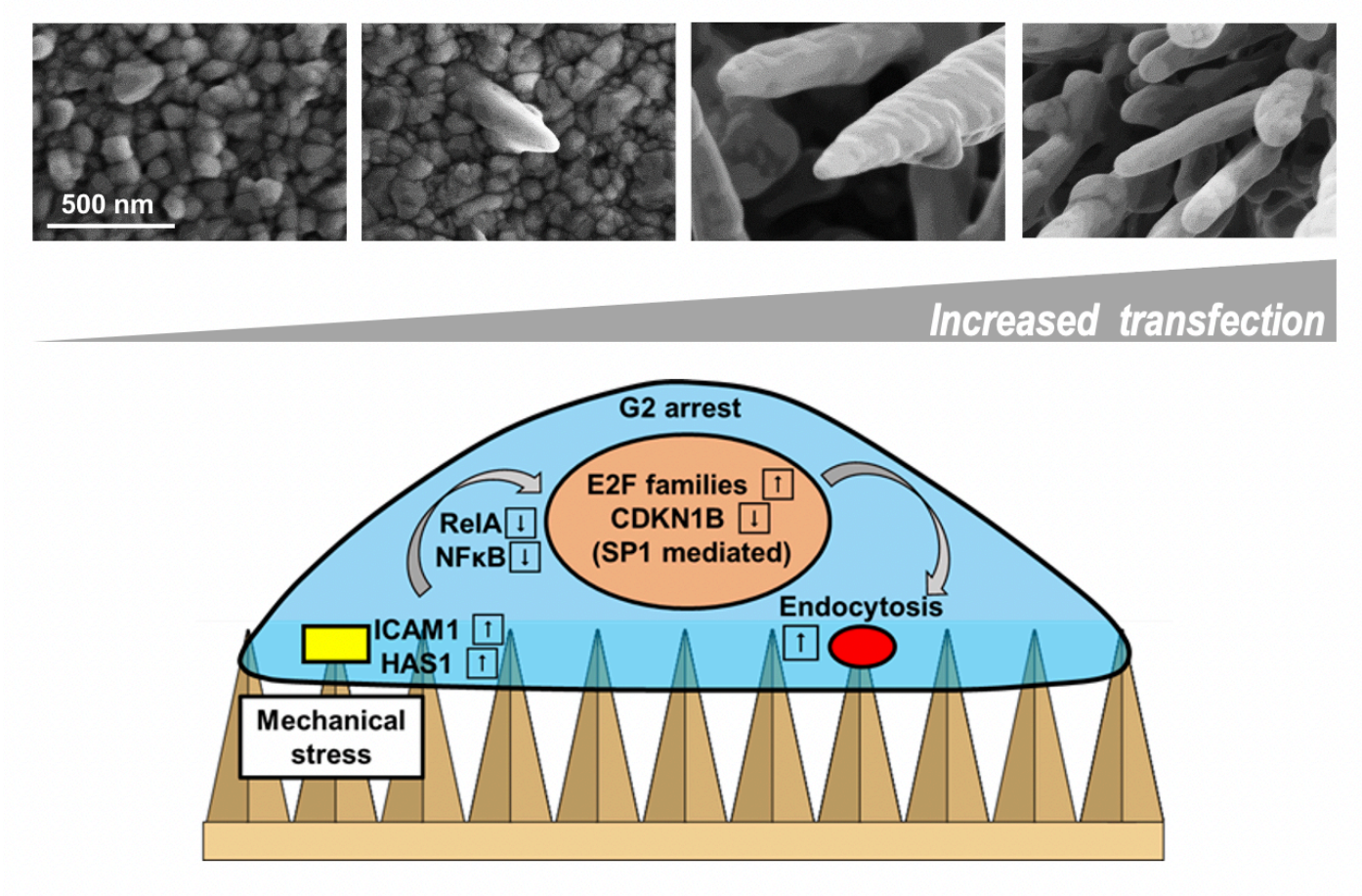
500 nm
Increased transfection
G2 arrest
E2F families
CDKN1B
(SP1 mediated)
RelA
NFκB
Endocytosis
ICAM1
HAS1
Mechanical stress

TOC Graphic